Two-dimensional fluctuation reflectometry : a comparison of analytical expressions for the Bragg back-scattering by localized perturbations and numerical results from a full-wave code

G. Leclert[1], E.Z. Gusakov[2], I. Boucher[3], M. Colin[3], S. Hacquin[3], S. Heuraux[3], F. Clairet[4], B.O. Yakovlev[2] and XL Zou[4]

[1] *LPIIM, UMR 6633 CNRS-Univ. Provence, C. 321, 13397 Marseille Cedex 20, France*
[2] *Ioffe Physico-Technical Institute, Polytekhnicheskaya 26, St Petersburg 194021, Russia*
[3] *LPMI, U. CNRS 7040, UHP Nancy I, BP 239, 54506 Vandoeuvre Cedex, France*
[4] *CEA-DRFC, CE Cadarache, 13108 St Paul-lez-Durance Cedex, France*

Introduction

The 2D theory of fluctuation reflectometry has been developed over the last years. The starting point is the work of Gusakov and co-workers [1] which gives a general integral expression for the signal scattered by a small amplitude density fluctuation. At the same time, 2D full-wave codes [2,3]have been developed. They have increased their capability at modelling physical systems of fairly large sizes, as well as their accuracy. It is now possible to make quantitative comparisons between the theory and the numerical results, at least in specific cases where the general expression can be worked out This turns out to be interesting in two respects: first, this cross-check gives more confidence for both approaches, and second the full-wave code can then be used to study the influence of large amplitude perturbations of any shape.

The two-dimensional theory of fluctuation reflectometry.

We restrict the study to the ordinary mode reflectometry. The plasma has an equilibrium linear density profile in the radial direction, with a density gradient length L. There are density fluctuations in the radial and poloidal directions, $n = n_{cr}(1 + x/L) + \delta n(x, y)$. x=0 is the position of the cut-off layer, where the density is n_{cr}. The electric field E_z of the O-mode obeys the 2D Helmholtz equation

$$\partial^2 E_z/\partial x^2 + \partial^2 E_z/\partial y^2 - (x/L + \delta n/n_{cr})E_z = 0 \quad (1)$$

In the Born approximation, the signal detected at the receiver, for a unit incident power, can be expressed [1] as

$$A_s(\omega) = \frac{2e^2 l^2}{mc^2}\int \frac{dk_y d\kappa dq}{(2\pi)^3} f(k_y) f(q-k_y) C(\kappa, q, k_y) e^{i\Psi} \delta n(q,\kappa) \quad (2)$$

$C(\kappa, q, k_y)$ is the scattering efficiency given for $\kappa L \gg 1$ by the asymptotic expression

$$C = -2\pi\sqrt{i\pi/\beta}\exp\left\{i\left[\beta^3/12 - \beta\sigma - \delta/4\beta\right]\right\} \quad (3)$$

$$\beta = \kappa L, \quad \delta = \ell^4 q^2 (q-2k_y)^2, \quad \sigma = -\ell^2\left[k_y^2 + (q-k_y)^2\right], \quad \ell = (Lc^2/\omega^2)^{1/3}$$

$f(k_y)=2(\pi\rho)^{1/2}\exp(-k_y^2\rho^2/2)$ is the antenna diagram, supposed to be Gaussian and Ψ is the phase of scattered wave for the probing in direction of the density gradient.
We choose density perturbations in the form of a poloidal island, namely

$$\delta n(x,y) = \delta n_0 \exp\left[-(x-x_f)^2/w_x^2\right]\exp\left[-(y-y_f)^2/w_y^2\right]\cos(qy) \qquad (4)$$

δn_0 is the perturbation amplitude. The perturbation is centred at (x_f, y_f), w_x and w_y are its spatial widths in the x and y directions, and q gives the poloidal density modulation.
Then the expression (2) can be solved by the saddle point method. This results in a complicated expression of the general form

$$A_S \approx \delta n G \sum_{n=\pm 1}\left\{\frac{\exp[-F(k_1)]}{\left(w_y^2 + 2iL/k_0\right)} + \frac{\sqrt{2}}{i}\frac{\exp[-F(k_2)]}{\left(w_y^2 + 2ix_f/k_0\right)}\right\} \qquad (5)$$

where G, k_1, k_2, $F(k_1)$ and $F(k_2)$ depend on the plasma and wave parameters.
The figure 1 gives the evolution of the amplitude $|A_S|$ of the detected signal, in the Born approximation, equation (2), as the centre (x_f, y_f) of the density perturbation moves through the plasma. For the case shown, the parameters are L=21, $w_x = w_y = 4$, $q = 0.35$ (lengths are normalised to the vacuum wavelength and wavevectors to the vacuum wavevector). The behaviour shown in Fig.1 is in agreement with the analytical result (5).
There are obviously two distinct responses. This can be interpreted in the following way. The first exponential term in equation (5) represents the contribution of the Bragg resonant scattering from the central component of the fluctuation spectrum, possessing poloidal wave number q and radial wave number $\kappa = 0$ (where the Bragg condition is satisfied for some oblique ray). The second exponential term represents the contribution of the small angle scattering by the side components of the perturbation spectrum. The first contribution is significant when the perturbation is located near the oblique cut-off for the ray such that $q = \pm 2k_y$, in this case the scattered wave propagates back and is picked up by the horn. The second term is substantial along the lines connecting the horn and the oblique cut-offs for the rays such that $q = \pm 2k_y$, ho wever it is maximal near intersection of these lines at the horn due to interference effect.

The numerical modelling of the wave-plasma system.
Several 2D full-wave codes have been designed for the purpose of reflectometry [2]. The present code [3] is based on a finite-difference scheme for the Helmholtz equation. The error is of the fourth order in the grid step, which allows a good accuracy with a reasonable number of points per wavelength (usually 10 to 12). The complex electric field is computed at every point of a rectangular box. Absorbing conditions [4] are imposed at the box boundaries to avoid spurious reflections of the outgoing wave. The emitting waveguide and horn are modelled as metallic surfaces where the electric field vanishes. The signal due to the density perturbation in the waveguide is determined by standard SWR methods.

Comparison of the results.
Variation with the amplitude
Since the analytical theory relies upon the Born approximation, the result depends linearly on the perturbation amplitude. Hence we have first to check this linear dependence for the numerical results. Figure 1 shows the amplitude of the received signal when the amplitude of a density perturbation at a fixed position is increased. The dependence is obviously linear as long as the relative amplitude is below 1.2%. Most results shown hereafter have been obtained for $\delta n/n_{cr} = 10^{-3}$. We shall come back on the nonlinear effects at the end of the section.

Variation with the poloidal wavenumber

In the expression (5) the q dependence is quite strong, because some terms in the second exponential depend on the 4th power of q. Hence, the small angle scattering term decays very strongly when the wavenumber increases. Figure 3 shows the 2D map of the amplitude of the received signal versus the position (x_f, y_f) of the density perturbation, obtained from the full-wave code, for the same case as Figure 1. The two responses (Bragg and small angle scattering) are clearly seen. An analysis of the data of Figures 1 and 3 shows that the locations of the Bragg peaks are in a good agreement: $7.4\lambda_0$ for analytical and $7.3\lambda_0$ for numerical. The small angle scattering response is however more important in the numerical computation than the analytical prediction.

Several values of the poloidal number between q = 0.25 and q = 0.6 have been compared. For q = 0.25 the Bragg peaks are located at $5.6\lambda_0$ (analytical) and $5.8\lambda_0$ (numerical). The Bragg scattering efficiency decreases by a factor of 10 from q=0.25 to q=0.6. As predicted, the decrease of the small angle scattering effect is much stronger.

The evolution of the signal amplitude As with the density gradient length L or the radial and poloidal widths w_x and w_y has also been checked. We have found a qualitative agreement between the analytical predictions and the numerical results.

Nonlinear effects.

The full-wave code can be run for perturbation amplitudes where the Born approximation is no longer valid. The figure 4 shows the 2D map of the amplitude of the detected signal for a density perturbation amplitude of 3%. The small angle scattering response is increased, and at the same time a significant signal is detected near the cut-off on the horn axis.

Conclusion.

The present study shows that a two-dimensional analytical study of the signal scattered by density perturbations can give quantitative predictions in a fair agreement with the results of a full-wave code. There are still differences. For example, the small angle scattering response seems to be more localised in the numerical results. In this region (perturbation close to the horn) the accuracy of the analytical model is weaker. It must also be noted that the antenna pattern is not gaussian in the simulations. The kind of perturbations which have been studied here can model MHD-like perturbations, where some large scale coherence exists. The results of both the analytical model and the code show that 2D effects can play a role in fluctuation reflectometry. The response is sensitive to the smaller values of the poloidal wavenumber, as in the 1D case for the radial fluctuations. However, the small angle scattering effect can induce a signal from regions far from the cut-off at a non negligible level. The code has also shown that nonlinear effects modify the response for fluctuation amplitudes above 2%, with a response enhancement along the horn axis.

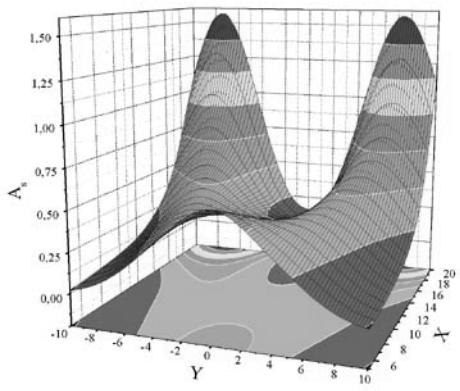

Figure 1 – Evolution of As versus (x_f, y_f). Case q = 0.25. Analytical result.

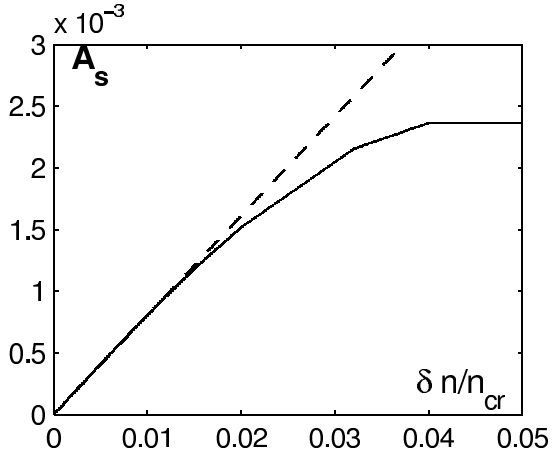

Figure 2 – Variation of the As versus δn ___: code, ----: linear dependence.

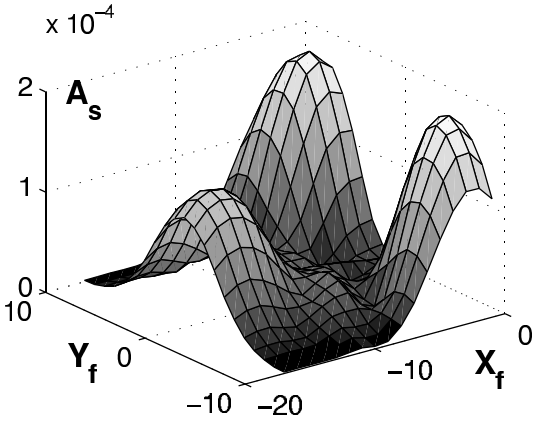

Figure 3 – 3D map of A_s versus (xf, yf): numerical computation. Same case as Figure 1.

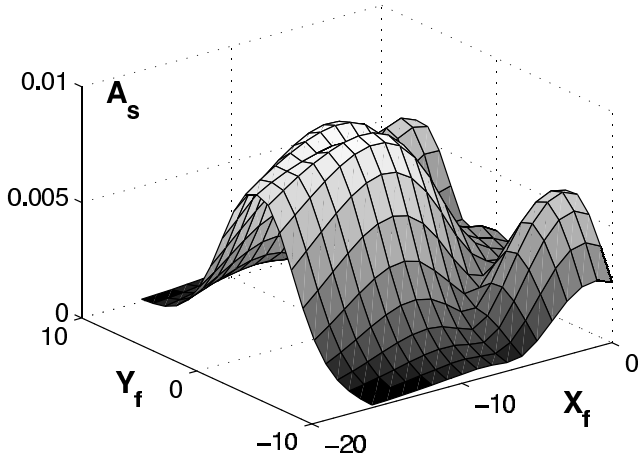

Figure 4 – 3D map of A_s versus (xf, yf): numerical computation. Nonlinear regime, $\delta n/n_{cr}$ = 0.03

References.

[1] E.Z. Gusakov, M.A. Tyntarev 1997, Fusion Engineer. Design **34-35**, 501

[2] J.H. Irby, Hornes, I.H. Hutchinson, P. Stek 1993 Plasma Phys. Control. Fusion **35**, 601

[3] C. Fanack *et al* 1995, 22 EPS Conf. Control. Fusion Plasma Phys. **19**C, IV-409

[4] R.L. Higdon 1986 Math. Comput. **47**, 437